Acta Cryst. (1962). **15**, 260

Electron Diffraction Intensities from Polycrystalline Material Containing Heavy Atoms

By J. M. Cowley and Shigeya Kuwabara*

Division of Chemical Physics, C.S.I.R.O. Chemical Research Laboratories, Melbourne, Australia

(*Received* 1 *November* 1960)

It is shown that the phase-grating approximation to the theory of electron diffraction developed by Cowley & Moodie (1957) can be applied to estimate the deviations of electron-diffraction intensities from the predictions of the kinematical theory for polycrystalline specimens with or without preferred orientation.

Measurements made on patterns obtained from oriented thin crystals of bismuth oxychloride, BiOCl, reveal that the relative intensities of the *hk*0 arcs differ from those expected from the kinematical theory and depend on the angle of tilt between the axis of preferred orientation (the *c*-axis) and the electron beam.

Detailed calculations of the relative intensities on the basis of the phase-grating approximation show good agreement with the measured values when suitable assumptions are made as to the average thickness and spread in thickness of the crystals and the range of angular misorientation of the crystals.

Comparison with the phase-grating approximation suggests that the Blackman formula, commonly used as a basis for the correction of intensities for dynamic effects, may fortuitously give a reasonable account of the variation of relative intensities with thickness when only a small range of atomic numbers is involved, but may be grossly wrong in the magnitudes and signs of the variations when atoms of widely differing atomic number are present.

1. Introduction

Analyses of crystal structures by electron-diffraction methods (reviewed, for example, by Cowley & Rees, 1958) have, with few exceptions, been based on the kinematic theory of electron diffraction. It has long been realized that except in very favourable cases, electron-diffraction intensities are liable to be modified by dynamic scattering effects, and in recent years several techniques have been evolved for 'correcting' intensities for the resultant deviations from kinematic scattering (Honjo & Kitamura, 1957; Nagakura, 1957; Vainstein, 1957; Vainstein & Lobachev, 1956). These techniques have as their basis the formulas derived by Blackman (1939) from the two-beam approximation to the dynamical theory, giving the intensities of reflections as functions of crystal thickness and electron wavelength. Experimental tests of these formulas have been made, for example, by Kuwabara (1955, 1957) and Honjo & Kitamura (1957) who observed the variation of intensity with crystal size and electron wavelength for thin films of simple metals and ionic compounds, and obtained general agreement with Blackman's theory.

However the two-beam approximation can be regarded as adequate only for very thick crystals, i.e. for crystals whose thickness is very much greater than the critical thickness for which deviations from kinematic scattering become important. When applied to thin crystals, as in Blackman's treatment, it is inapplicable for two important reasons. Firstly, as the crystal thickness decreases, the probability that only two strong beams (the incident beam and one diffracted beam) will exist in the crystal also decreases and there is considerable evidence that, especially if heavy atoms are present, many strong beams exist simultaneously for most orientations of crystals which are thick enough for deviations from kinematic scattering to be appreciable. Secondly, no account is taken of the possible differences in phase of scattering from atoms of different atomic number within a unit cell. It is this omission which led to the false conclusion that the kinematic theory represents the limiting case of the dynamic theory for very small thicknesses.

A more realistic treatment of the diffraction from thin crystals requires a suitable formulation of the *n*-beam dynamical diffraction theory. This was achieved by Cowley & Moodie (1957) who applied their new formulation of physical-optics theory (Cowley & Moodie, 1958) and considered a crystal to be divided into a very large number of thin slices. In a first set of approximations to their general results they derived a formula giving the diffraction amplitudes as sums of single, double, and other-multiple scattering terms. This formula was later derived from the starting point of the more conventional form of the dynamic theory

* On leave from the Hiroshima University, Hiroshima, Japan.

by Fujiwara (1959), using the generalized Born approximation and by Fujimoto (1959) using a matrix theory. In his discussion of the transition from dynamical to kinematical intensities, Miyake (1959) made use of the results of Fujiwara & Fujimoto in showing that the kinematical theory represented the correct limiting case for $\lambda H \rightarrow 0$, where H is the crystal thickness, but not for $H \rightarrow 0$. This point is made clearer by considering the second type of approximation made by Cowley & Moodie (1957, 1959) in which the diffraction by a crystal is approximated by successive subdivision into an increasing number of phase-gratings. In the first of these approximations, valid for very thin crystals, the crystal is approximated by a single phase-grating. The effect of the crystal on an incident beam is to multiply the wave function by

$$q(x, y) = \exp\{i\sigma\varphi(x, y)\}, \quad (1)$$

where

$$\sigma = 2\pi m\lambda/h^2$$

and

$$\varphi(x, y) = \int_0^H \varphi(x, y, z)\,dz,$$

i.e., $\varphi(x, y)$ is the projection of the potential distribution of the crystal in the beam direction, taken to be the z axis. The diffraction pattern is then given by the Fourier transform of $q(x, y)$. The kinematical approximation is valid only if the exponent in (1) is very much smaller than unity so that we can write

$$q(x, y) = 1 + i\sigma\varphi(x, y)$$

and

$$\mathscr{F}q(x, y) = \delta(\xi, \eta) + i\sigma\Phi(\xi, \eta),$$

where $\Phi(\xi, \eta)$ is the kinematical structure factor and ξ, η are reciprocal space coordinates. The delta function represents the transmitted, undeflected beam. The minimum thickness which one can reasonably consider is the diameter of one atom. Since for commonly used wavelengths most atoms have complex atomic scattering factors with appreciable phase angles (Ibers & Hoerni, 1954), the exponent of (1) is not always small and the kinematic approximation can be made only for light atoms. The kinematic approximation could be considered as generally valid only for $\lambda H \rightarrow 0$ which would ensure a sufficiently small exponent.

For a single layer of atoms the pseudo-kinematic theory of Hoerni (1956) would be appropriate, since it would give essentially the same result as equation (1). For more than a single layer of atoms there would be some overlapping of atoms in the projection $\varphi(x, y)$ and the scattering could no longer be expressed in terms of complex atomic scattering factors of individual atoms. The pseudo-kinematic theory then fails, but the expression (1) remains valid and gives a good approximation for all thicknesses small enough for Fresnel diffraction effects within the crystal to be unimportant (i.e. so that the Ewald sphere can be approximated by a plane: in practice, for thicknesses less than about 100 Å). The calculation of diffraction intensities from the phase-grating approximation of the Cowley–Moodie theory is very simple and straightforward in principle, although possibly laborious in practice. One first calculates the projection in the beam direction, $\varphi(x, y)$, of the potential distribution of the diffracting object, then finds the values of $\cos\varphi(x, y)$ and $\sin\varphi(x, y)$ and forms their Fourier transforms. The method is not limited to the consideration of periodic objects but for our present purposes we assume the specimen to be composed of crystals which can be considered periodic in at least two directions.

For a perfect single crystal of uniform thickness the projection $\varphi(x, y)$ is relatively simple only if the beam is parallel to a principal axis of the crystal. It is periodic for all beam directions. The values of the cosine and sine may be calculated at sufficiently small intervals of x and y over one unit cell of the projection and the structure factors and intensities of the diffraction spots are then found by summing the Fourier series with these values as coefficients. For polycrystalline samples it is possible to make the usual assumption that there is no coherence between the beams diffracted by different crystallites, i.e. that all crystallites diffract independently. The intensity at any point of the diffraction pattern is the sum of the intensity contributions from all crystallites. One should, in principle, make a single crystal calculation, as above, for each value of the crystal thickness and crystal orientation present in the polycrystalline sample and sum all the results, properly weighted. Although in practice some reasonable approximations can be made to simplify this process, it is not possible to make the assumption of the kinematical theory, or the two-beam dynamical theory, that the orientation of the crystal affects the intensity of a reflection only in as much as it determines the 'excitation error', or distance of the Ewald sphere from the reciprocal-lattice point.

The most direct test of validity of the phase-grating approximation would be given by observing the change in the intensities of the spot pattern when a single crystal is tilted with respect to the electron beam. This is impracticable because of the severe experimental difficulties involved in obtaining, manipulating and maintaining a single crystal sufficiently thin, uniform and undistorted. We have therefore chosen to use polycrystalline samples having a preferred orientation.

Suppose that for all crystallites one particular crystal axis is oriented parallel to a given direction such as, for example, the normal to a supporting film, and that otherwise their orientations are random. For convenience, we call the axis of preferred orientation the c-axis. If the electron beam is inclined at an appreciable angle to this axis, we obtain an 'oblique-texture' arc pattern in which the $hk0$ arcs appear

along the zero layer-line through the origin. The orientation of the particular crystallites which contribute to any one arc for a given tilt is then completely determined, apart from a few ambiguities, and varies with the angle of tilt between the beam and the orientation axis. For each angle of tilt the projection $\varphi(x, y)$ can be calculated for the crystals giving each reflection. Since for a given tilt the projections corresponding to each arc will be different and these projections will vary in different ways with the tilting angle, the relative intensities of the arcs calculated on the phase-grating approximation will vary with tilting angle.

In this the phase-grating approximation differs from all other approximations which may conveniently be applied. The kinematical theory and Hoerni's pseudo-kinematical theory both predict that the intensity of $hk0$ arcs, for example, should be independent of tilting angle. The two-beam dynamical theory also would give constant $hk0$ intensities except for the effect of an increase in effective crystal thickness. Our considerations must therefore be of considerable significance in connection with the use of intensities from 'oblique texture' electron-diffraction patterns for purposes of structure analysis.

It is evident that the changes in relative intensities of the reflections should be enhanced by the presence of heavy atoms, especially if light atoms are also present, since then the various maxima of the projection $\varphi(x, y)$ will differ widely in the phase change which they produce. With this in mind we have obtained patterns from oriented aggregates of thin lamellar crystals of bismuth oxychloride, BiOCl, measured the relative intensities of the $hk0$ arcs for a number of tilting angles, and compared the results with calculations using the phase-grating approximation.

2. Experimental

BiOCl crystals are tetragonal with space group $P4/nmm$–D_{4h}^{7}. The cell dimensions and the atomic positions are given (Wyckoff, 1948) as follows (cf. Fig. 1):

$$a_0 = 3{\cdot}883 \text{ Å}, \quad c_0 = 7{\cdot}348 \text{ Å}$$

O (a) 000; $\frac{1}{2}\frac{1}{2}0$;
Cl (c) $0\frac{1}{2}u$; $\frac{1}{2}0\bar{u}$, $u = 0{\cdot}645$;
Bi (c) $0\frac{1}{2}u$; $\frac{1}{2}0\bar{u}$, $u = 0{\cdot}170$.

Lamellar polycrystals of BiOCl were prepared by the following procedures. A small quantity of $BiCl_3$ was dissolved in conc. HCl. The clear solution was poured into a beaker containing water. Then BiOCl was formed as a white milky precipitate. The crystal size could be controlled by changing the temperature of the water or the concentration of the $BiCl_3$ solution. Drops of the suspension were dried on nickel grids covered with evaporated carbon films. The two specimens for which intensity measurements were made were formed with the water at 100 °C. For specimen A the $BiCl_3$ solution was dilute. For specimen B it was saturated.

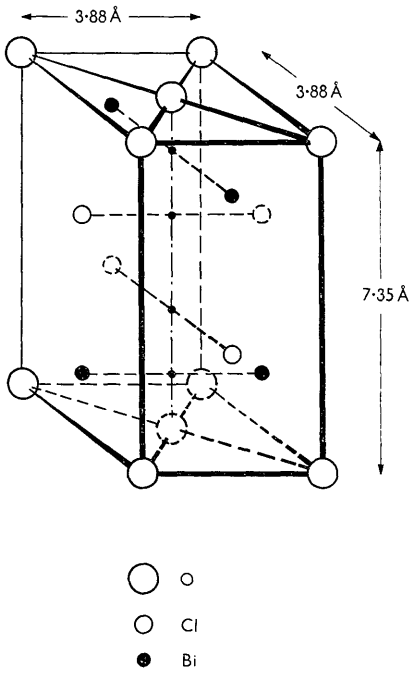

Fig. 1. The structure of BiOCl.

An electron-microscope study of the crystal forms was made using the Siemens Elmiskop I. From Fig. 2(a) it can be seen that the BiOCl crystals prepared by a method similar to that for specimen A have the form of very thin sheets, often crumpled or folded and sometimes forming irregular circular particles. The corresponding selected-area diffraction patterns showed extensive 'two-dimensional' arrays of spots such as in Fig. 2(b). A small proportion of the crystals gave diffraction patterns showing evidence of considerable disorder. The micrographs and selected area diffraction pattern, from specimen B, shown in Figs. 3(a) and 3(b) reveal thicker and more regular crystals, giving spot patterns limited in extent by 'three-dimensional' diffraction effects.

The electron-diffraction instrument used to obtain the patterns from polycrystalline specimens used for intensity measurements has a specimen-to-plate distance of 270 mm. and an accelerating voltage of 48 kV. Kodak Contrast Process Orthochromatic Plates, 4×10 inches, were used and developed in $D19(1:1)$ at 20 °C. for 4 min. Specimens were tilted through angles from 0° up to 25°, and 5 or 6 sets of photographs with different exposures were taken for each angle of tilt. Fig. 4 shows an example of the photographs obtained from specimen A. A Leeds & Northrup microphotometer was used to derive the density curve. The scanning was carried out in the direction parallel to the tilting axis through the central spots of the patterns. The so-called Schwarzchild–Villiger (1906) effect was removed carefully. Intensity measurements

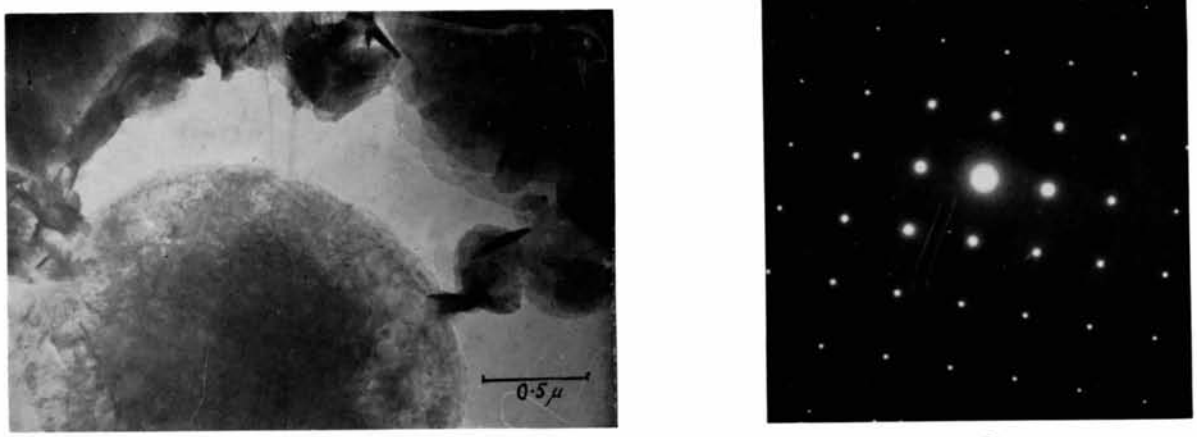

(*a*) (*b*)

Fig. 2. Electron micrograph, (*a*), and selected area diffraction pattern, (*b*), of a BiOCl specimen similar to specimen *A*.

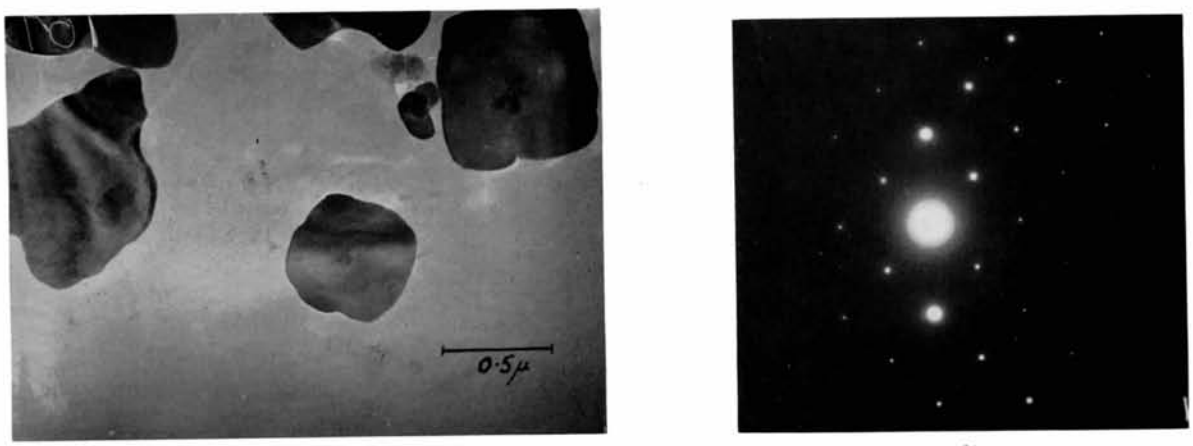

(*a*) (*b*)

Fig. 3. Electron micrograph, (*a*), and selected area diffraction pattern, (*b*), of BiOCl specimen *B*.

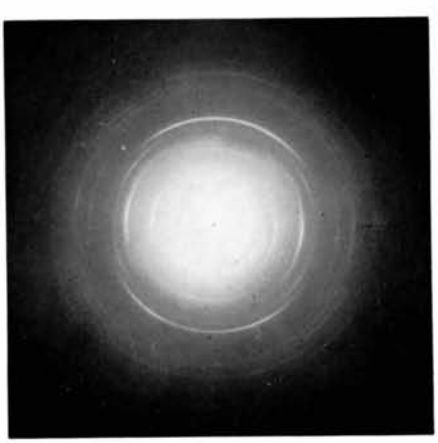

Fig. 4. Electron diffraction pattern from polycrystalline BiOCl specimen with crystals oriented about an axis tilted at an angle of 25° to the electron beam.

[*To face p.* 262

of the diffraction patterns were made using the method of Karle & Karle (1950). The intensity versus density curves were found to be linear up to a density $D=0{\cdot}8$ (Fig. 5).

The relative intensities for various angles of tilt, obtained from the experiment with specimen *A* are shown in Table 1 and Fig. 6, where the 220 intensity was normalized to 1·00. Fig. 6 also contains the experimental points for specimen *B*. The mean error of the experiment was about 5% except for systematic errors such as that arising in the subtraction of a smooth background from the microphotometer trace.

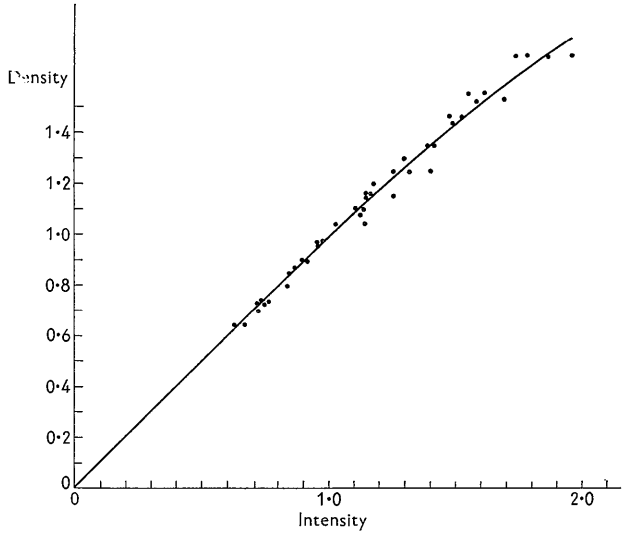

Fig. 5. One of the calibration curves of density *vs.* intensity for a Kodak Contrast Process Orthochromatic plate exposed to 48 kV. electrons, showing the spread of experimental points.

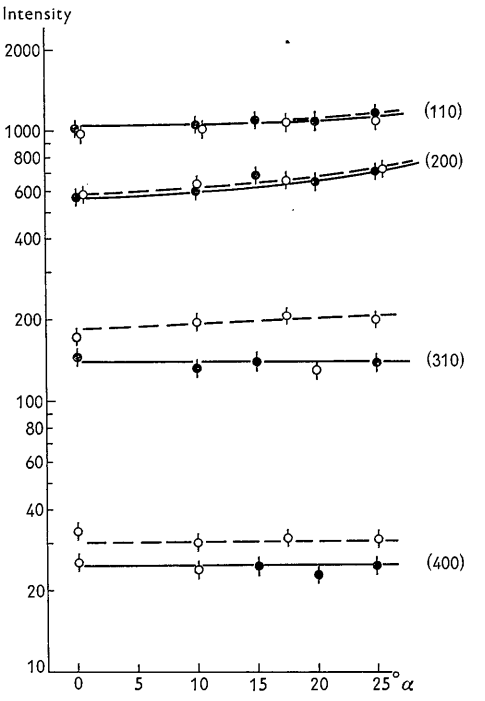

Fig. 6. The variation of relative intensities with angle of tilt measured for BiOCl specimens giving patterns such as Fig. 2. The 220 reflection is normalized to 100. Filled circles: specimen *A*. Open circles: specimen *B*.

Table 1. *Experimental intensity ratios for hk*0 *reflections of* BiOCl, *sample A, for various angles of tilt*

The columns 1 to 6 refer to six separate measurements of different plates.

Angle (°)	(*hk*0)	1	2	3	4	5	6	Mean
0	110	961	1043	1028	1066	1210	1014	1054 ± 39
	200	519	581	582	600	650	584	586 ± 17
	220	100	100	100	100	100	100	100
	310	148	147	146	151	154	162	151 ± 2
	400	28	28	27	34	25	23	28 ± 2
10	110	940	1025	—	911	1030	—	976 ± 30
	200	520	550	763	561	623	—	603 ± 43
	220	100	100	100	100	100	—	100
	310	135	136	158	118	138	—	137 ± 5
	400	24	22	36	23	23	—	25 ± 3
15	110	1061	1330	1025	1113	948	1294	1129 ± 62
	200	682	908	665	666	612	745	711 ± 43
	220	100	100	100	100	100	100	100
	310	132	117	132	157	157	158	142 ± 7
	400	21	25	—	34	34	26	28 ± 3
20	110	1005	1358	920	1091	1084	1111	1095 ± 60
	200	618	700	549	627	677	727	650 ± 26
	220	100	100	100	100	100	100	100
	310	129	149	139	126	122	135	133 ± 4
	400	23	26	22	19	21	31	24 ± 2
25	110	1270	1241	1114	1400	1076	1400	1250 ± 56
	200	781	722	652	866	634	788	741 ± 36
	220	100	100	100	100	100	100	100
	310	183	173	126	142	120	148	149 ± 10
	400	26	31	26	27	17	25	25 ± 2

As is shown in Fig. 6, intensities of the 310 and 400 reflections are almost independent of the tilting angle, but those of 110 and especially 200 reflections show definite increases.

3. Calculation of intensities

In our approximation the structure factors can be obtained by a one-dimensional Fourier transform of a projection of the exponential function in equation (1). For example, $h00$ reflections will be obtained when the electron beam is very nearly parallel to the 100 planes. With respect to the orthogonal set of x, y, z axes, the beam is in the z-axis direction and tilting is assumed to take place about the x-axis. Then $h00$ reflections will be given by crystallites for which the a-axis of the crystal coincides with the x-axis. The projection of the potential distribution on the xy plane will then vary as illustrated in Fig. 7. For the $x=0$ plane the variation of $\varphi(0, y)$ with y will show very large excursions for zero tilt but only small fluctuations for an arbitrary angle of tilt.

Although the integral of $\varphi(0, y)$ over y will be the same in both of these cases, the integrals of $\exp\{i\sigma\varphi(0, y)\}$ may differ considerably. Similarly for other x values. Hence the projection of the exponential function on the x-axis will vary with tilting angle and the relative intensities of the $h00$ reflections, given by Fourier transform of this projection, will vary likewise.

To simplify calculations, different a and b axes are taken for each $hk0$ reflection and its higher orders, in such a way that with respect to the new axes each $hk0$ reflection becomes an $h00$. Thus for the 110 and 220 reflections, unit cell axes $2^{\frac{1}{2}}$ times as great as the normal cell axes are chosen and these reflections become the 200 and 400 respectively. Similarly the 310 becomes the 10,0,0 reflection of a unit cell with axes $10^{\frac{1}{2}}$ times as great. The coordinates of the projection of any atom of the crystal with respect to the projection of these axes may then be calculated from simple geometric arguments.

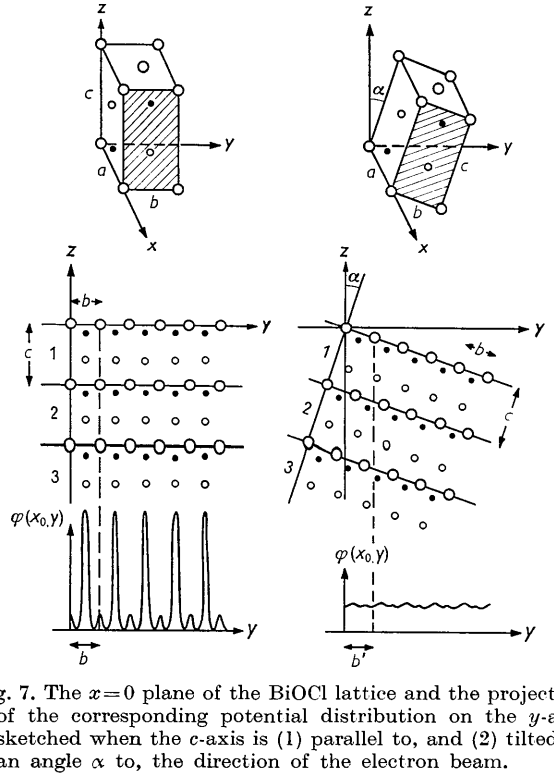

Fig. 7. The $x=0$ plane of the BiOCl lattice and the projection of the corresponding potential distribution on the y-axis sketched when the c-axis is (1) parallel to, and (2) tilted at an angle α to, the direction of the electron beam.

The first step in calculating the projections $\varphi(x, y)$ must necessarily be to determine the projection of the potential distribution of each kind of atom present. The projection is obtained by taking the Fourier transform of the atomic scattering factor. For convenience we use standard Fourier-series methods, and make the assumption that all atoms have the same temperature factor, namely $B=1{\cdot}0$ Å^2. The projection of the potential energy for one unit cell is given by

$$\varphi'(x, y)=(c_0/v_0)\sum_h\sum_k \Phi^K_{hk}\exp\{-B(\sin^2\theta)/\lambda^2\} \times\exp\{-2\pi i(hx+ky)\}, \quad (2)$$

where $v_0=a_0b_0c_0$, the volume of the unit cell, and Φ^K_{hk} is the kinematic structure factor, given by

$$\Phi^K_{hk}=\sum_i g_i.\exp\{2\pi i(hx_i+ky_i)\}, \quad (3)$$

where g_i is the atomic scattering factor for electrons. The potential-energy projection for each atom is found by assuming the structure to consist of only one atom per unit cell, situated at the origin. Then (2) becomes

$$\varphi'(x, y)=(c_0/v_0)\sum_h\sum_k g_{hk}.\exp\{-B(\sin^2\theta)/\lambda^2\} \times\exp\{-2\pi i(hx+ky)\}. \quad (4)$$

The summation was made for Bi, O and Cl atoms, using the values of $f_e[=(2\pi me/h^2)g]$ given by Vainstein (1953), and adding terms up to $hk0=860$, i.e. to $(\sin\theta)/\lambda=1{\cdot}3$ Å^{-1}. The results for $h00$ reflections and zero tilting angle, plotted at intervals of 1/60 of the unit cell, are shown in Fig. 8. For other reflections the axes are expanded with respect to the distribution, since a larger unit cell is used. For non-zero tilting angle the y-axis is contracted with respect to the distribution because the axis of tilt is always taken to be the x-axis. The results are expressed as phase shifts in degrees, i.e. values of $(180/\pi)\sigma\varphi'(x, y)$, using the value of σ appropriate for 48 ke.V., i.e. $\sigma=1{\cdot}20\times10^{-3}$ Å^{-1}, e.V.$^{-1}$. It may be noted that the maximum phase shift is 97° for Bi, 30° for Cl and 14° for O. It is evident then that the kinematical approximation must be poor for a crystal no more than one unit cell thick.

The projection of the potential for the whole crystal is next calculated by summing the projections of the potentials for all atoms in the crystal, thus:

$$\varphi(x, y)=\sum_i[\varphi_i'(x, y)*\delta(x-x_i, y-y_i)].$$

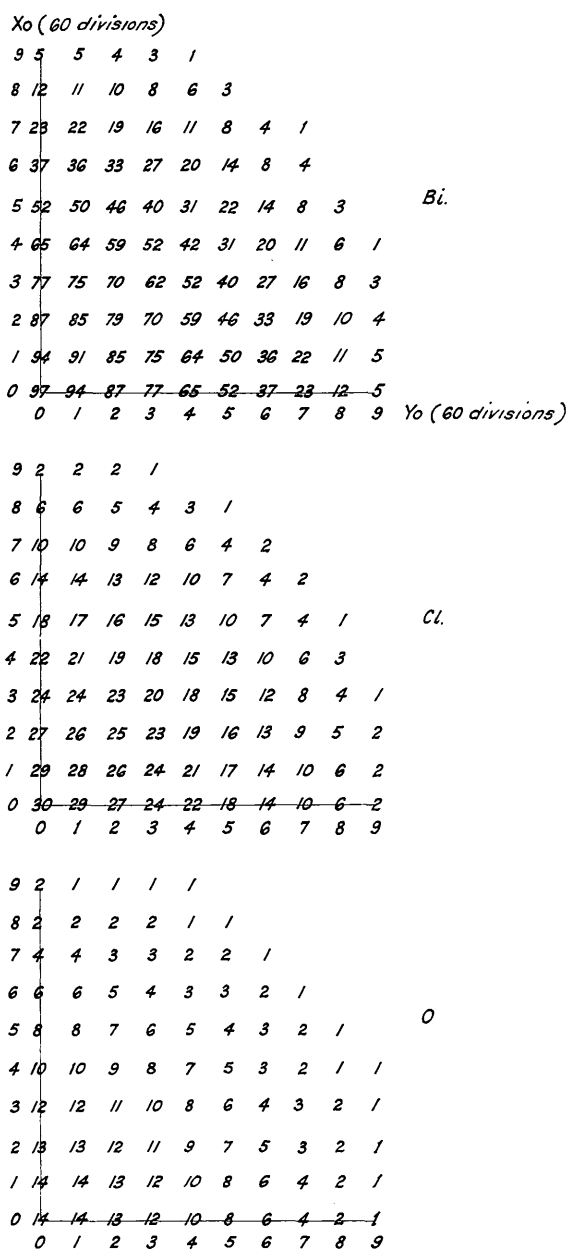

Fig. 8. Values of the projection of the potential distribution of individual Bi, O and Cl atoms at intervals of 1/60th of the axes of the BiOCl unit cell. The units are degrees of phase shift.

The summation is in practice carried out for all atoms of the crystal whose projections lie within one unit cell of the projection $\varphi(x, y)$.

The structure factor is then given, from equation (1) by

$$\Phi_{hk} = \iint [\cos \sigma\varphi(x, y) - 1] . \exp \{2\pi i(hx+ky)\} . dx . dy + i \iint \sin \sigma\varphi(x, y) . \exp \{2\pi i(hx+ky)\} . dx . dy \quad (5)$$

The transmitted beam has been removed by subtracting unity in the first integral.

Since for each reflection the unit cell is chosen to

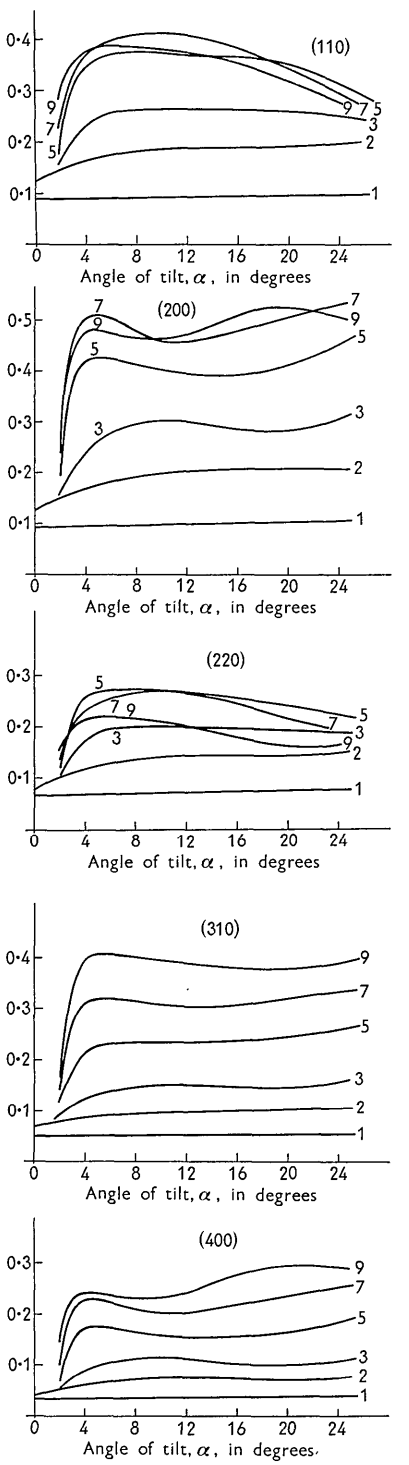

Fig. 9. The calculated variation of structure amplitude with angle of tilt for the first five $hk0$ reflections of BiOCl. Curves are drawn for crystal thicknesses corresponding to from 1 to 9 molecular layers of BiOCl, i.e. from 1 to 9 unit cells.

Table 2. *Structure amplitudes calculated for hk0 reflection of* BiOCl *for various thicknesses (in units of molecular* BiOCl *layers) and various tilting angles*

Layer numbers	(*hk*0)	2°*	5°	10°	17·5°	25°	Layer numbers	(*hk*0)	2°	5°	10°	17·5°	25°
1	110	0·087	0·090	0·093	0·097	0·100	6	110	0·215	0·373	0·406	0·374	0·296
	200	0·093	0·094	0·101	0·104	0·111		200	0·221	0·506	0·461	0·454	0·503
	220	0·067	0·070	0·072	0·076	0·078		220	0·122	0·257	0·286	0·251	0·206
	310	0·048	0·048	0·051	0·052	0·055		310	0·120	0·273	0·270	0·285	0·299
	400	0·033	0·034	0·036	0·039	0·039		400	0·081	0·219	0·196	0·186	0·223
2	110	0·123	0·172	0·186	0·191	0·199	7	110	0·247	0·384	0·411	0·374	0·280
	200	0·132	0·180	0·201	0·206	0·213		200	0·244	0·507	0·463	0·493	0·534
	220	0·084	0·130	0·143	0·147	0·155		220	0·133	0·251	0·274	0·233	0·188
	310	0·069	0·091	0·099	0·103	0·109		310	0·140	0·317	0·306	0·316	0·336
	400	0·041	0·066	0·073	0·074	0·077		400	0·103	0·226	0·200	0·226	0·256
3	110	0·162	0·255	0·264	0·265	0·251	8	110	0·284	0·409	0·396	0·370	0·258
	200	0·163	0·268	0·301	0·282	0·311		200	0·260	0·493	0·462	0·507	0·523
	220	0·107	0·192	0·202	0·199	0·191		220	0·150	0·253	0·243	0·212	0·176
	310	0·094	0·136	0·151	0·146	0·161		310	0·172	0·360	0·353	0·356	0·367
	400	0·053	0·102	0·113	0·102	0·115		400	0·127	0·228	0·212	0·252	0·272
4	110	0·171	0·301	0·331	0·330	0·302	9	110	0·310	0·386	0·382	0·344	0·262
	200	0·175	0·357	0·353	0·350	0·403		200	0·267	0·477	0·460	0·520	0·497
	220	0·104	0·221	0·248	0·238	0·228		220	0·153	0·216	0·210	0·173	0·174
	310	0·113	0·182	0·199	0·190	0·205		310	0·170	0·409	0·398	0·380	0·398
	400	0·056	0·137	0·136	0·131	0·157		400	0·149	0·241	0·234	0·289	0·288
5	110	0·188	0·370	0·373	0·364	0·302	10	110	0·320	0·336	0·333	0·309	0·267
	200	0·197	0·426	0·402	0·402	0·463		200	0·274	0·455	0·431	0·493	0·458
	220	0·108	0·270	0·272	0·255	0·221		220	0·140	0·159	0·150	0·127	0·186
	310	0·120	0·228	0·232	0·242	0·261		310	0·188	0·432	0·427	0·392	0·443
	400	0·066	0·175	0·159	0·158	0·192		400	0·165	0·257	0·221	0·297	0·302

* For 1 and 2 layers, 2° should be read to be 0 degree.

make the reflection an $h00$, and since the projections are all centrosymmetric, equation (5) can be simplified to give

$$\Phi_{hk} = \iint [\cos \sigma\varphi(x, y) - 1] . \cos 2\pi hx . dx . dy + i \iint \sin \sigma\varphi(x, y) . \cos 2\pi hx . dx . dy . \qquad (6)$$

The projection $\varphi(x, y)$ for BiOCl was calculated for all thicknesses from 1 to 10 unit cells, i.e. from 1 to 10 of the BiOCl composite layers, and for five different tilting angles from 0 to 25 degrees. For each projection the integrals

$$\int [\cos \sigma\varphi(x, y) - 1] dy \quad \text{and} \quad \int \sin \sigma\varphi(x, y) dy$$

were calculated at regular intervals of x, and the integrals of (6) were approximated by summations in the usual way to give, finally, the values of the structure factors Φ_{hk}. The values of $|\Phi_{hk}|$ are listed in Table 2 and plotted as functions of angle in Fig. 9.

When the number of layers is large and the angle of tilt is very small or zero the above calculation becomes difficult because the gradient of the potential projection $\varphi(x, y)$ becomes very great in small regions of the projection and the cosine and sine functions fluctuate rapidly, requiring a much finer subdivision of the unit cell. However in these cases the integral of the cosine and sine functions becomes very small and the contributions to the structure factors can be neglected.

From Fig. 9 it is seen that the structure factors do vary considerably not only with thickness but also with the angle of tilt. However these results cannot be directly compared with experiment because they apply to the idealized case of perfectly oriented crystals of uniform thickness. For comparison with the experimental results it is necessary to take account of the distributions in thickness and orientation.

For convenience these distributions can be approximated by Gaussian functions so that the mean values of the intensities are given by

$$\overline{\Phi^2_{hk}} = \iint D(H, \alpha) . \Phi^2_{hk} . dH . d\alpha , \qquad (7)$$

where

$$D(H, \alpha) = D(H) . D(\alpha) ,$$
$$D(H) = \exp \{-a_H (\Delta H)^2\} ,$$
$$D(\alpha) = \exp \{-a_\alpha (\Delta\alpha)^2\} ,$$

and ΔH and $\Delta\alpha$ are the deviations of thickness (in number of layers) and orientation angle of the crystals from the mean values. The values of the constants a_H and a_α, chosen as giving reasonable representations of the experimental conditions for specimen A, are

$$a_H = 0{\cdot}10, \; a_\alpha = 0{\cdot}01 \text{ deg.}^{-2}$$

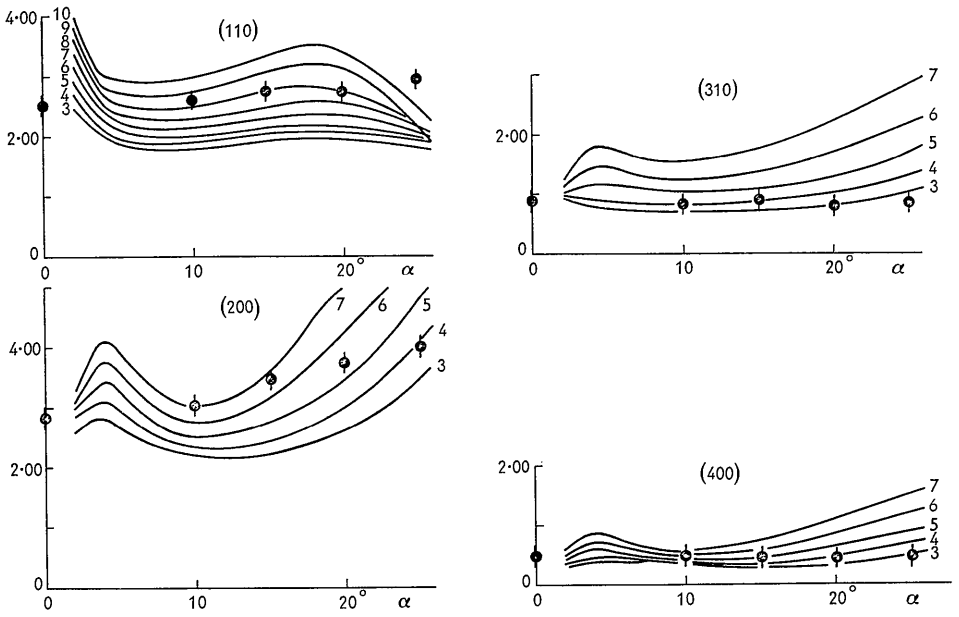

Fig. 10. The calculated variation of relative intensities of *hk*0 reflections of BiOCl with angle of tilt, averaging over a range of thickness by applying the distribution function $D(H)$ of equation (7). The 220 reflection intensity is normalized to 1·00.

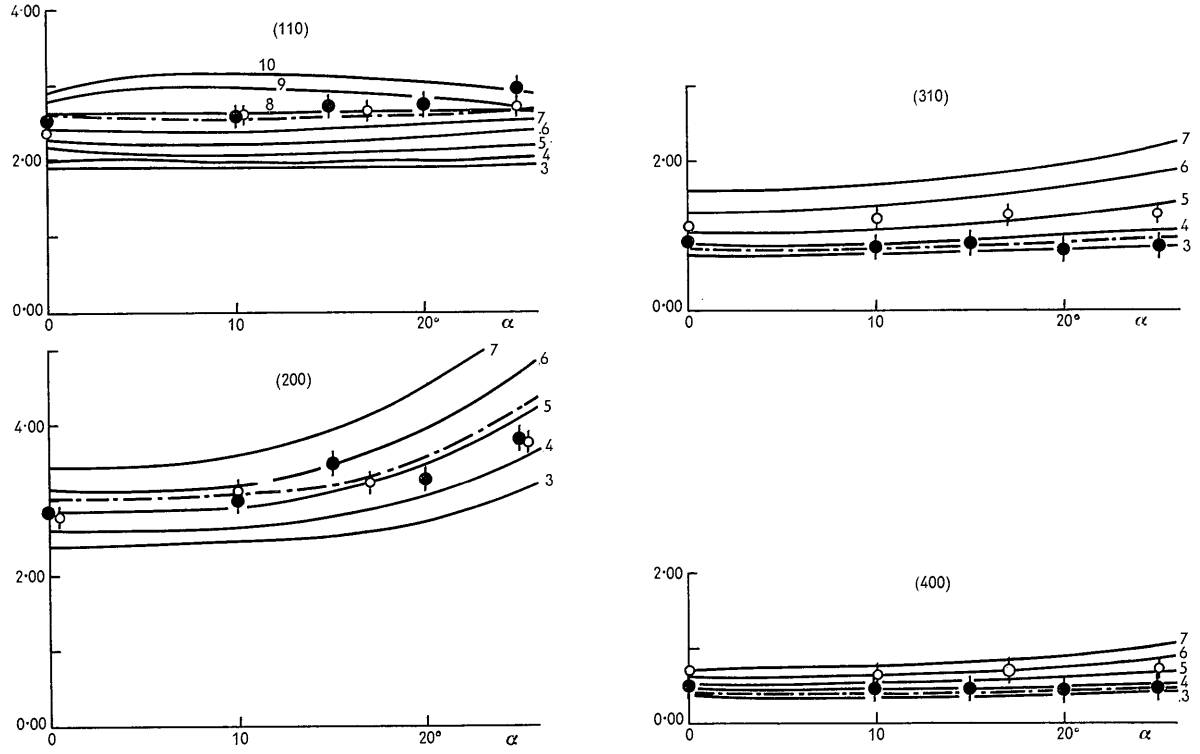

Fig. 11. The calculated variation of relative intensities of the *hk*0 reflections of BiOCl with angle of tilt, taking into account the distributions of crystal thickness and tilt by using the distribution function $D(H, \alpha)$ of equation (7). The 220 reflection normalized to 2·00. The experimental points are shown, filled circles for specimen *A* and open circles for specimen *B*. The chain lines correspond to the calculated values for an average thickness of 4 layers and an artificial temperature factor with $B' = 1{\cdot}2$ Å.

so that $D(H)$ is reduced to 10% for $\Delta H = 4$ layers and $D(\alpha)$ is reduced to 10% for $\Delta\alpha = 15°$.

Performing the integration of (7) over H gives the variation of intensities with tilting angle shown in Fig. 10. Here the intensities have been normalized by taking the value for the 220 reflection equal to 1·00, since experimentally only relative intensities were measured. Finally, integrating over α gave the set of relative intensities as functions of mean tilting angle, shown and compared with the experimental values in Fig. 11.

It can be seen from Fig. 11 that there is general agreement between the theoretical and experimental results from specimen A except that the experimental results appear to agree with theoretical curves corresponding to different thicknesses for the different reflections. Thus the best agreement seems to be for 8–9 layers for the 110 reflection, 5–6 layers for the 200 and 3–4 layers for the 310 and 400.

This can be explained as follows. In our calculations the integration over the angle made allowance for the spread in orientations in rotation about the x axis, but no allowance has been made for a similar spread for rotations about the y axis. To take such rotations into account fully would involve a prohibitively large amount of calculation. However a reasonable approximation can be made. An angular distribution about the y axis would have the effect of broadening the peaks of the projection of the potential distribution. The influence of such a broadening can be taken into account by introducing an artificial temperature factor in the one-dimensional Fourier summations in the x-direction. The average intensities can therefore be expressed as

$$\overline{\Phi_{hk}^2} = \iint D(H, \alpha) . \Phi_{hk}^2 \exp\{-B' (\sin^2\theta)/\lambda^2\} . dH . d\alpha \, . \tag{8}$$

The best agreement with experiment was found by assuming the mean thickness to be equivalent to 4 layers and an artificial temperature factor with $B' = 1{\cdot}2$ Å. The chain lines in Fig. 11 show the values of relative intensities calculated with these assumed values. The agreement with experiment is now good.

An alternative interpretation of the apparent variation of the mean number of layers with the reflection, shown in Fig. 11, is based on the theory of Cowley (1961) concerning the effects of bending or distortion of crystals on diffraction patterns. It has been shown that if, within regions of the specimen which can be considered to diffract coherently under the existing experimental conditions, the crystals are appreciably bent, or there is a variation in orientation of parts of the crystals, the effective crystal size in the beam direction is thereby decreased. It may be that the apparent average crystal thickness of about 4 layers is in fact given as a result of bending or mis-orientation of thicker crystals. If appropriate assumptions concerning the nature of the bending are made, including an assumption of a Gaussian distribution of crystal orientations, the intensity of a reflection may be expressed as

$$I(\mathbf{s}) = \sum_i W_i(\mathbf{s}) . \exp(2\pi i \mathbf{r}_i . \mathbf{s}) \times \exp\{(-\pi^2/c^2)(s . r_i . \cos\beta_i)^2\} , \tag{9}$$

where $\mathbf{s}$ is a vector in reciprocal space, $\mathbf{r}_i$ is the vector, of magnitude r_i, from the origin of the Patterson function to a Patterson peak for which the scattering factor is $W_i(\mathbf{s})$, and β_i is the angle between the vector $\mathbf{r}_i$ and the z axis. The final exponential term modifies the Patterson function by a Gaussian distribution in the z direction. The width of the Gaussian distribution, and hence the effective crystal thickness, is inversely proportional to $\mathbf{s}\,(=\frac{1}{2}d_{hk0})$.

The values of the effective thickness, deduced from Fig. 11 are plotted against the s values appropriate to the various reflections in Fig. 12. They are seen to lie, within experimental error, on a hyperbola, thus confirming that equation (9) does, in fact, account for the observed effect to a good approximation.

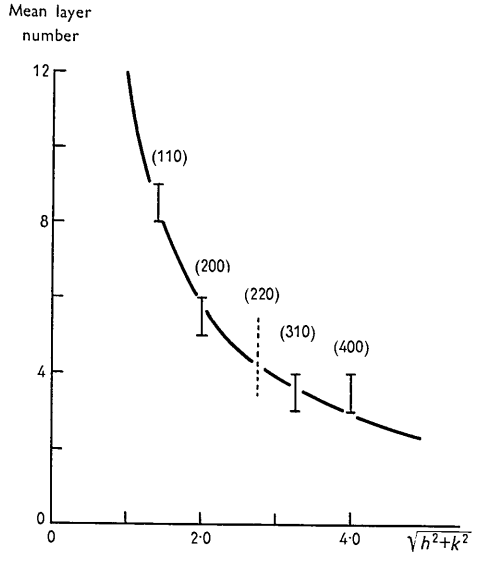

Fig. 12. The apparent mean number of layers, deduced from Fig. 11 plotted against the magnitude of the reciprocal lattice vector and compared with a hyperbolic curve.

For specimen B the effective thickness deduced from the curves for the 310 and 400 reflections in Fig. 11 is almost twice that for specimen A. The calculations have not been extended to cover the thickness range (12–15 layers) in which the corresponding effective thickness for the 110 and 200 reflections might be expected. However it seems probable that the agreement with experiment in this case may not be as good as for specimen A. This is not surprising since, for the thicknesses involved (ca. 100 Å), the two-dimensional phase-grating approximation cannot be expected to be very good. Diffraction patterns

such as Fig. 3(*b*) provided evidence that three-dimensional diffraction effects are, in fact, important in this case.

4. Discussion

We have shown that the observed variation of the intensity of electron-diffraction reflections with angle of tilt can be adequately explained on the basis of the phase-grating approximation of the Cowley–Moodie theory. The theoretical results, such as those illustrated in Fig. 9, indicate that the variation of the intensities with tilting angle would be much more pronounced if specimens had been used in which the spread of orientations was less. Further experimental results are required in order to establish the range of validity of the phase-grating approximation.

The methods used to calculate the intensities involve a number of approximations for which the range of validity has not been explored. Thus the approximation of assuming the crystal to be represented by a single phase grating breaks down for a thickness and in a manner which have not been fully investigated. Also the introduction of the temperature factor in equation (2) and of the artificial temperature factor in equation (8) cannot readily be justified since the use of a kinematical temperature factor is wrong in principle for a phase object. These approximations were made in order to avoid the enormously greater amount of labour otherwise involved. They are probably justified in that the errors they introduce are probably less than those generated by the necessity to make assumptions concerning the spreads in crystal size and orientation.

Since the methods which have been used to date to calculate departures from kinematic scattering are based on formulas due to Blackman (1939), it is of interest to compare the predictions of the present theory with those of Blackman's. Firstly, of course, we have the result that for oriented polycrystalline samples the intensities vary with the angle of tilt whereas the two beam theory gives no such variation.

However if we make the assumption that the intensity for random orientation of the crystallites is proportional to the intensity at a particular, non-special, orientation we may compare the predictions as to variation of intensity with thickness.

According to Blackman's theory, the effective structure factor is given by

$$\Phi^B_{hk} \propto \Phi^K_{hk} \cdot \left[\frac{1}{A}\int_0^A J_0(2x)\,.\,dx\right]^{\frac{1}{2}}, \qquad (10)$$

where

$$A = (2\pi m/h^2)\,.\,|\Phi^K_{hk}|\,.\,H\lambda\,.$$

$J_0(2x)$ is the zero order Bessel function, and Φ^K_{kh} is the kinematic structure factor.

If we consider a crystal composed of Bi atoms only, placed, for convenience, at the O positions of the BiOCl lattice, the equation (10) and the phase-grating approximation give similar variations of the relative intensities with crystal thickness, as shown in Fig. 13. The deviations from the kinematic intensities are in the same direction and of approximately the same magnitude. The intensities for the phase grating approximation here are those calculated for an angle of tilt of 5°. Other angles of tilt would give deviations from the kinematic of different amounts but in the same direction.

If, however, the O and Cl atoms in the BiOCl lattice are taken into account, the relative phase of the scattering from Bi and O or Cl atom peaks in the projection has a large effect on the intensities in the phase grating approximation, so that the variation with thickness now differs greatly from that given by equation (10), being sometimes in the opposite direction, as shown in Fig. 14.

Experimental tests of Blackman's formula have to date been limited to crystals containing only one kind

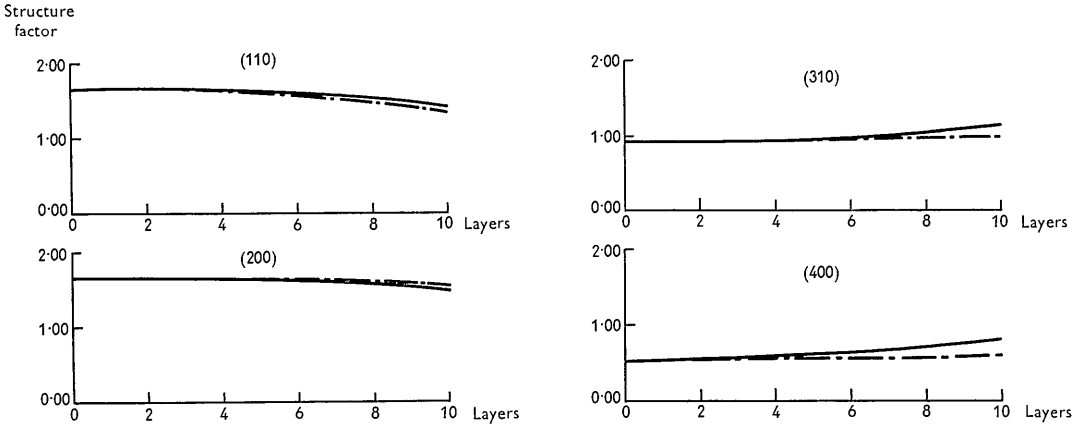

Fig. 13. Comparison of the variation of structure amplitude with thickness calculated from the phase-grating approximation (continuous lines) and from Blackman's theory (broken lines) for a hypothetical BiOCl-type lattice containing only Bi atoms, for an angle of tilt of 5 degrees.

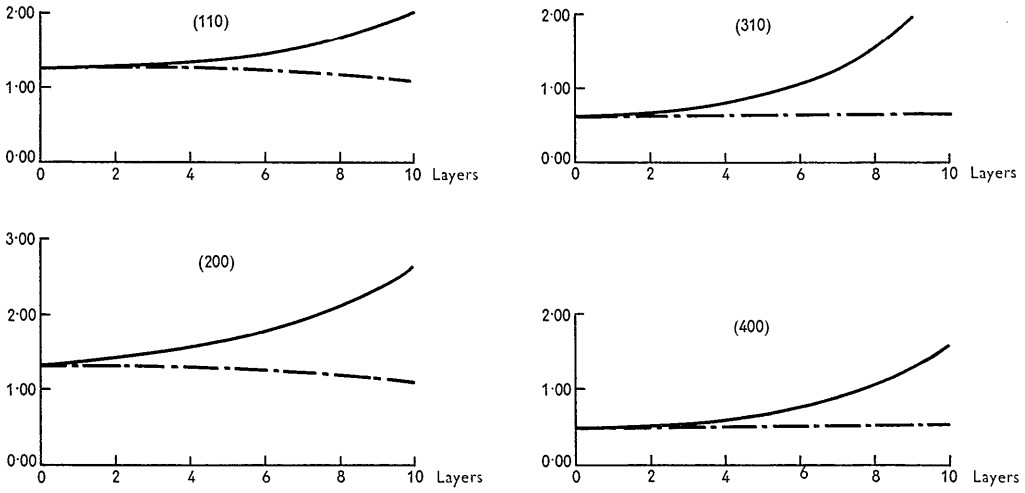

Fig. 14. As for Fig. 13, calculated for the BiOCl lattice.

of atom or else containing only light atoms. It is therefore not surprising that approximate agreement with the formula was found. Our calculations indicate that serious discrepancies would be found if both heavy and light atoms were present.

We wish to express our gratitude to Mr J. Farrant of this Division for the electron microscope study of our specimens.

One of the authors (S. K.) would like to express his sincere thanks to the C.S.I.R.O. for its kind offer of financial support for his stay in Australia.

References

Blackman, M. (1939). *Proc. Roy. Soc.* A, **173**, 68.
Cowley, J. M. (1961). *Acta Cryst.* **14**, 920.
Cowley, J. M. & Moodie, A. F. (1957). *Acta Cryst.* **10**, 609.
Cowley, J. M. & Moodie, A. F. (1958). *Proc. Phys. Soc.* **71**, 533.
Cowley, J. M. & Moodie, A. F. (1959). *Acta Cryst.* **12**, 360.
Cowley, J. M. & Rees, A. L. G. (1958). *Rep. Progr. Phys.* **21**, 165.
Fujimoto, F. (1959). *J. Phys. Soc. Japan*, **14**, 1558.
Fujiwara, K. (1959). *J. Phys. Soc. Japan*, **14**, 1513.
Hoerni, J. A. (1956). *Phys. Rev.* **102**, 1530.
Honjo, G. & Kitamura, N. (1957). *Acta Cryst.* **10**, 533.
Ibers, J. A. & Hoerni, J. A. (1954). *Acta Cryst.* **7**, 405.
Karle, J. & Karle, I. L. (1950). *J. Chem. Phys.* **18**, 957.
Kuwabara, S. (1955). *J. Phys. Soc. Japan*, **10**, 416.
Kuwabara, S. (1957). *J. Phys. Soc. Japan*, **12**, 637.
Miyake, S. (1959). *J. Phys. Soc. Japan*, **14**, 1347.
Nagakura, S. (1957). *Acta Cryst.* **10**, 601.
Schwarzchild, K. & Villiger, W. (1906). *Astrophys. J.* **23**, 284.
Vainstein, B. K. (1953). *J. Exp. Theor. Phys. USSR*, **25**, 157.
Vainstein, B. K. (1957). *Kristallografiya*, **2**, 340.
Vainstein, B. K. & Lobachev, A. N. (1956). *Kristallografiya*, **1**, 472.
Wyckoff, R. W. G. (1948). *Crystal Structures*, Vol. 1.